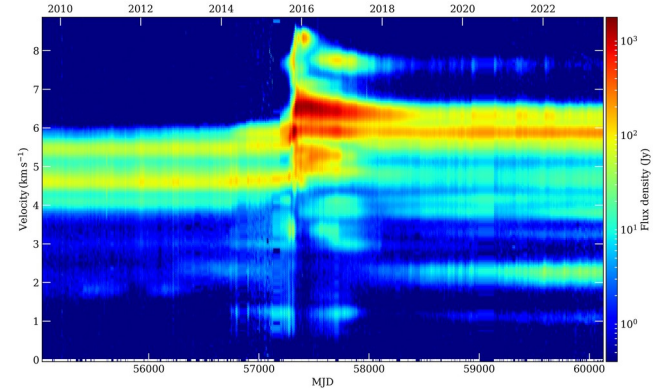


Studying Stellar Evolution and Mass Loss with Masers

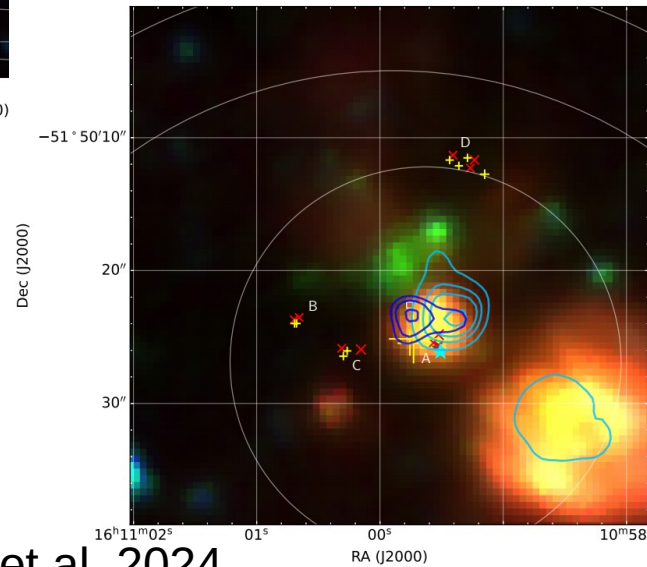
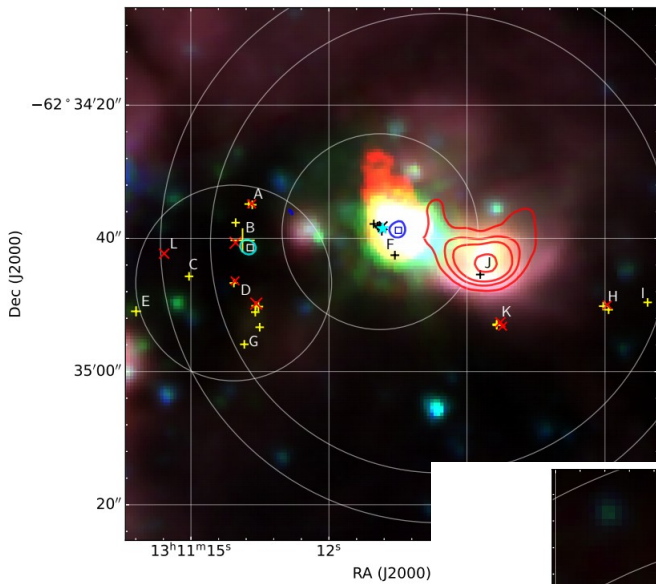
Anna Bartkiewicz



NICOLAUS COPERNICUS
UNIVERSITY
IN TORUŃ

Faculty of Physics, Astronomy
and Informatics

Masers are useful

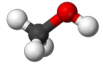


Voronkov et al. 2024

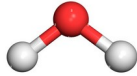
- Maser emission can escape from dense regions, close to the central objects that are not easily reachable at other wavelengths: star-forming regions and evolved stars.
- Being compact, bright, non-thermal emission structures they are ideal VLBI targets to be used for understanding physical parameters such as density and temperature, but also for accurate position measurements making them ideal astrometry targets (e.g., BeSSel, BAaDE, VERA, PMs) .
- Transitions at GHz – THz.
- Discovered in 60s.

Gray 2012: Maser emission is related to

- **Star formation**



methanol (CH₃OH) – class I, II



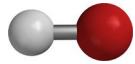
water (H₂O)



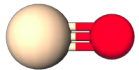
formaldehyde (H₂CO)



ammonia (NH₃)



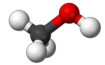
hydroxyl (OH)



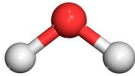
silicon monoxide (SiO)

Gray 2012: Maser emission is related to

- **Star formation**



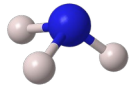
methanol (CH_3OH) – class I, II



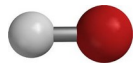
water (H_2O)



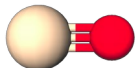
formaldehyde (H_2CO)



ammonia (NH_3)



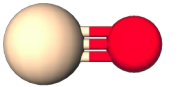
hydroxyl (OH)



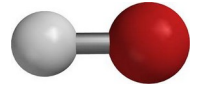
silicon monoxide (SiO)

- **Evolved stars (AGB, RSG)**

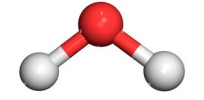
silicon monoxide (SiO)



hydroxyl (OH)

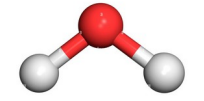


water (H_2O)

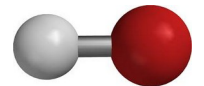


- **Planetary nebulae and pPN**

water (H_2O)



hydroxyl (OH)



IAUS in Kagoshima (March 2023)

Cosmic Masers: Proper Motion toward the Next-Generation Large Projects – ca. 160 participants.

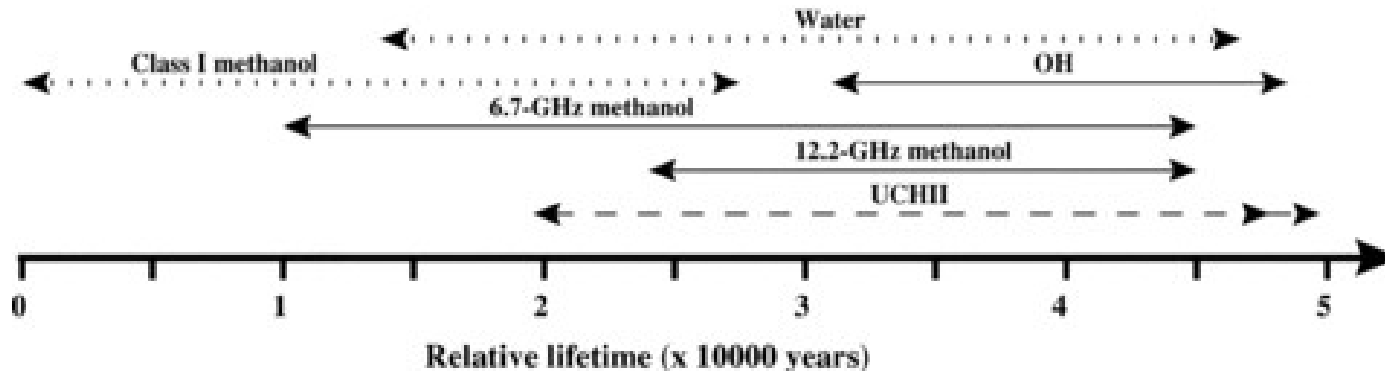


Star formation: surveys → evolutionary sequence

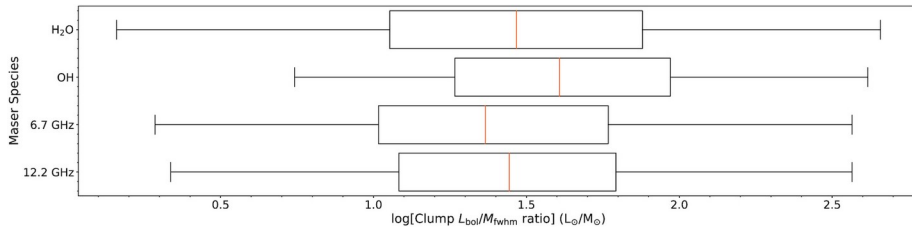
- Ellingsen (2007) searched for 6.7-GHz class II methanol masers towards 200 GLIMPSE: „Many of the target sources are at an evolutionary phase prior to that associated with 6.7-GHz methanol masers.” (‘straw man’ model)

- Breen et al. (2010)

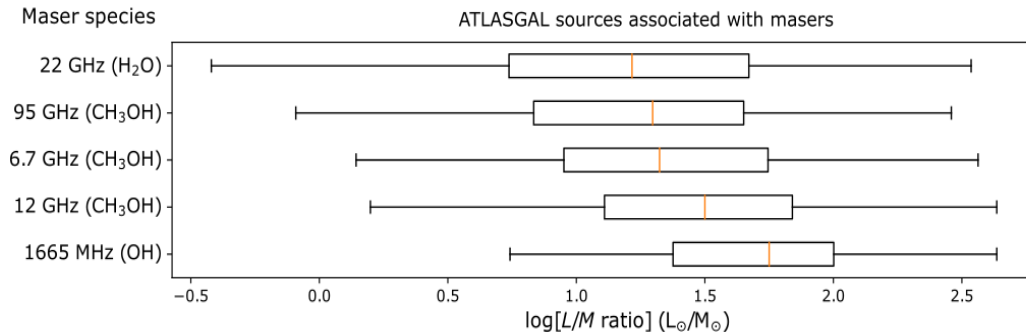
„We additionally find that **more luminous 6.7-GHz methanol masers are more likely to be associated with OH masers which are known to trace a generally later evolutionary phase of massive star formation than isolated methanol masers.** Therefore, we expect that there is a trend between 6.7-GHz methanol maser peak luminosity and evolutionary phase, with the more luminous 6.7-GHz methanol maser peaks tending towards a later phase in evolution than 6.7-GHz methanol masers with low peak luminosities.”



Star formation – evolutionary sequence questioned...



Billington et al. 2020: The conditions required for the production of maser emission only occur during a relatively narrow period during a star's evolution: $\sim 0.4\text{--}2 \times 10^4$ yr.



Early Star Formation Traced by Water Masers – Ladeyschikov 2024

„The results of the L/M ratio analysis depicted in Figure 1, revealed that 22 GHz H₂O masers appear earlier in the evolutionary sequence than clMM masers at 6.7, 12 GHz, and 1665 MHz OH masers. From the presented data **author concludes that 22 GHz water masers arise before 6.7 GHz methanol masers in the evolutionary sequence.** This conclusion is consistent with study Breen & Ellingsen (2011), but differed from several other studies (Ellingsen et al. 2007; Breen et al. 2010; Jones et al. 2020) that suggested water masers appear after the onset of 6.7 GHz methanol masers in the evolution timeline.”

Urquhart 2024: Evolutionary Trends in Star Formation

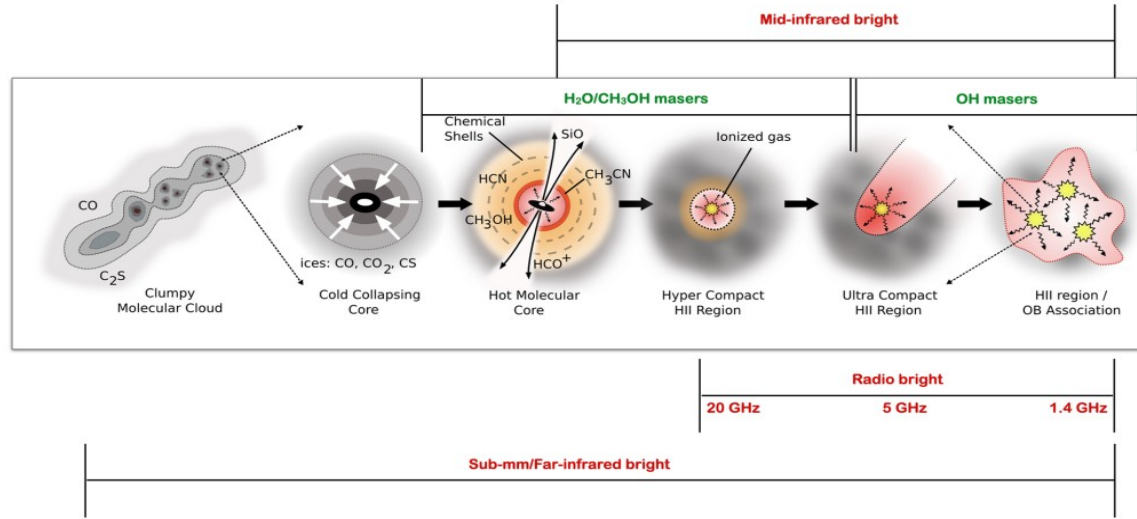


Figure 1. Schematic for the evolutionary sequence of massive star formation. Infrared and radio surveys are sensitive to the more evolved stages shown to the right while submillimetre surveys are sensitive to all evolutionary stages. The greyscale indicates the distribution of cold gas and dust with the darker areas corresponding to denser regions. The protostellar objects are indicated by the yellow circles, warmer gas by the orange colouring and the hotter ionized gas is shown in red. Molecular lines used to trace the properties of the molecular gas in different stages are also noted. The red labels and associated horizontal lines show the wavelengths and time ranges that different stages are observable, and the green labels indicate the maser associations. Image Credit: Cormac Purcell.

- Over the past 20 years, the Galactic plane has been surveyed at high resolution at wavelengths from 1 micron through to 20 cm. The combination of these surveys has produced large samples of deeply embedded young stars located across the Galactic disc.

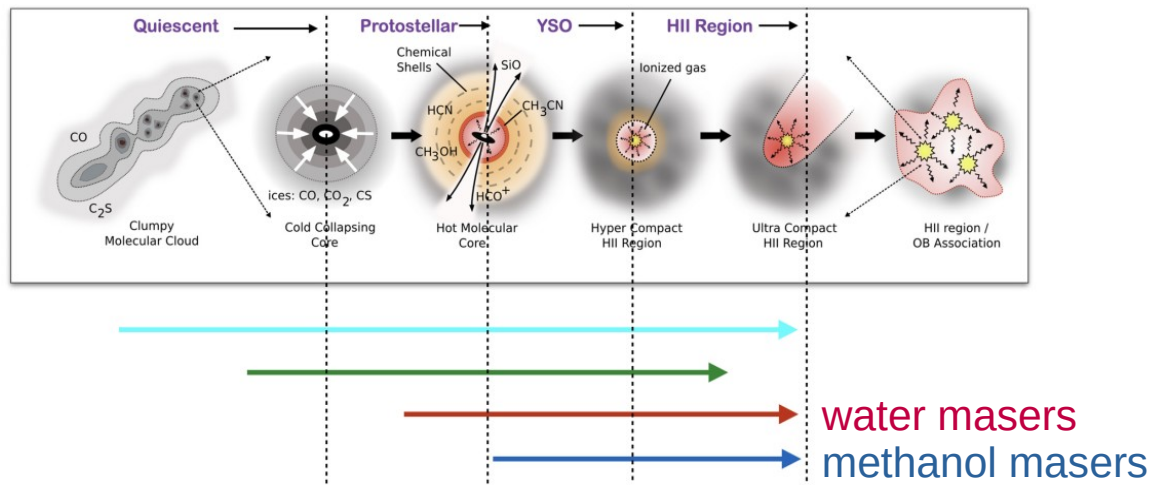


Figure 10. Schematic is the same as shown in Figure 1 but has been adapted to show approximately when the star formation tracers discussed in the text first appear and when they start to decline in frequency. The arrows correspond to outflows (top), EGOs (upper middle), water masers (lower middle) and methanol masers (bottom).

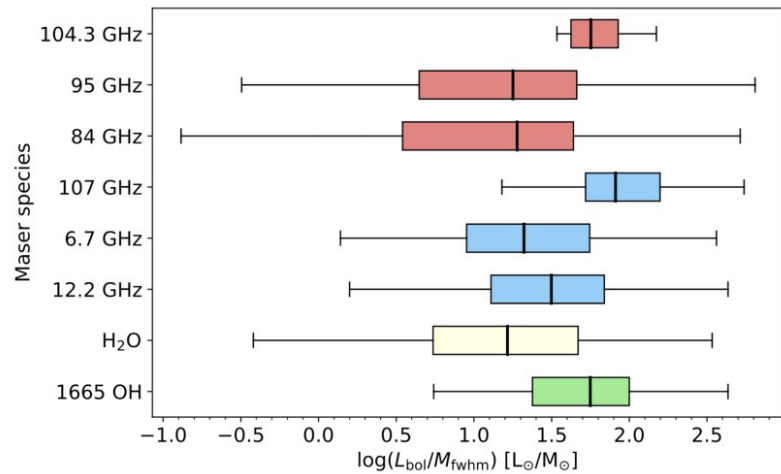


Figure 12. Box plot showing the distribution of $L_{\text{bol}}/M_{\text{fwhm}}$ -ratios for ATLASGAL clumps associated with a wide range of maser species. This plot has been produced using the results from Ladeyschikov *et al.* (2022) and Yang *et al.* (2023) and appears in Yang *et al.* 2023 (this proceeding) and reproduced here with their permission. Image Credit: Wenjin Yang.

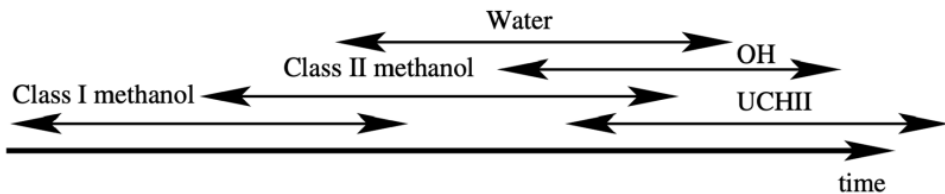


Figure 11. Model for an evolutionary sequence high-mass star formation regions constructed from maser emission. Image credit: This has been adapted from figure 2 of Ellingsen *et al.* (2007). Image Credit: Simon Ellingsen.

Multifreq. observations needed, e.g., Kang et al. 2024: Jet and Outflows in Massive Star Forming Region: G10.34–0.14

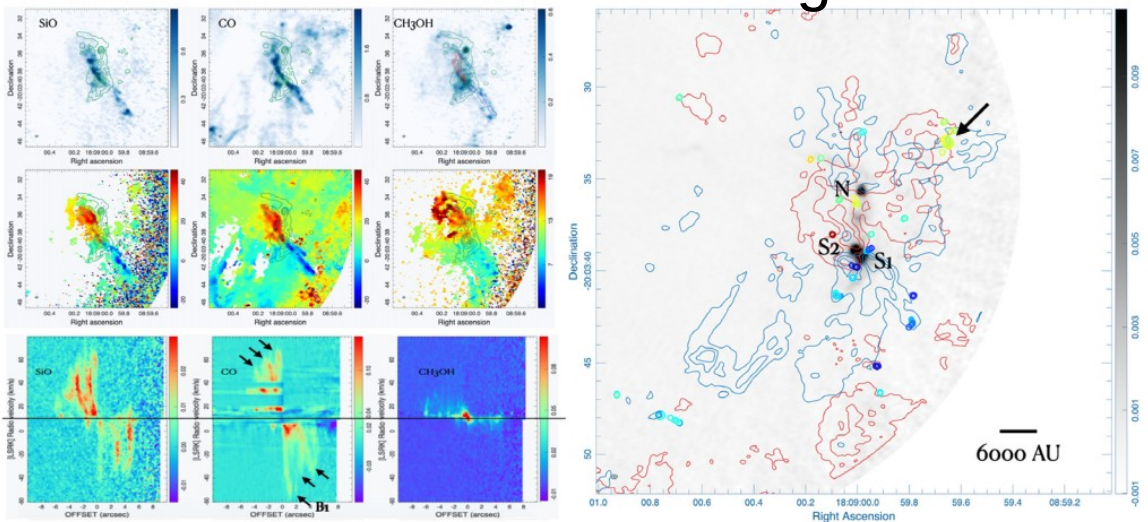


Figure 1. (Left) The top and middle images display moment 0 and 1 maps in SiO, CO, and CH₃OH from left to right. The continuum emission in green contours is overlaid on the moment maps of each molecular transitions. The HV CO jet ($30 < |V - V_{\text{sys}}| < 70 \text{ km s}^{-1}$) is presented with blue and red contours in the moment 0 map of CH₃OH. The PV diagrams along the collimated CO jet for each molecular lines are shown at the bottom. Note that the jet axis shown in the moment 1 map of CO differs slightly between the blue- and red-shifted components. The systemic velocity of $+11 \text{ km s}^{-1}$ is marked by a black horizontal line. The bullet-like features are indicated by black arrows. (Right) Blue- and red-shifted LV CO outflows ($7 < |V - V_{\text{sys}}| < 15 \text{ km s}^{-1}$) are overlaid on the 1.3 mm dust continuum emission. The open circles represent the positions of the 44 GHz methanol masers, adopted from [Cyganowski et al. \(2009\)](#). The symbol area corresponds to the intensity and the color indicates the velocity, ranging from $+7.8 \text{ km s}^{-1}$ (purple) to $+19.7 \text{ km s}^{-1}$ (red).

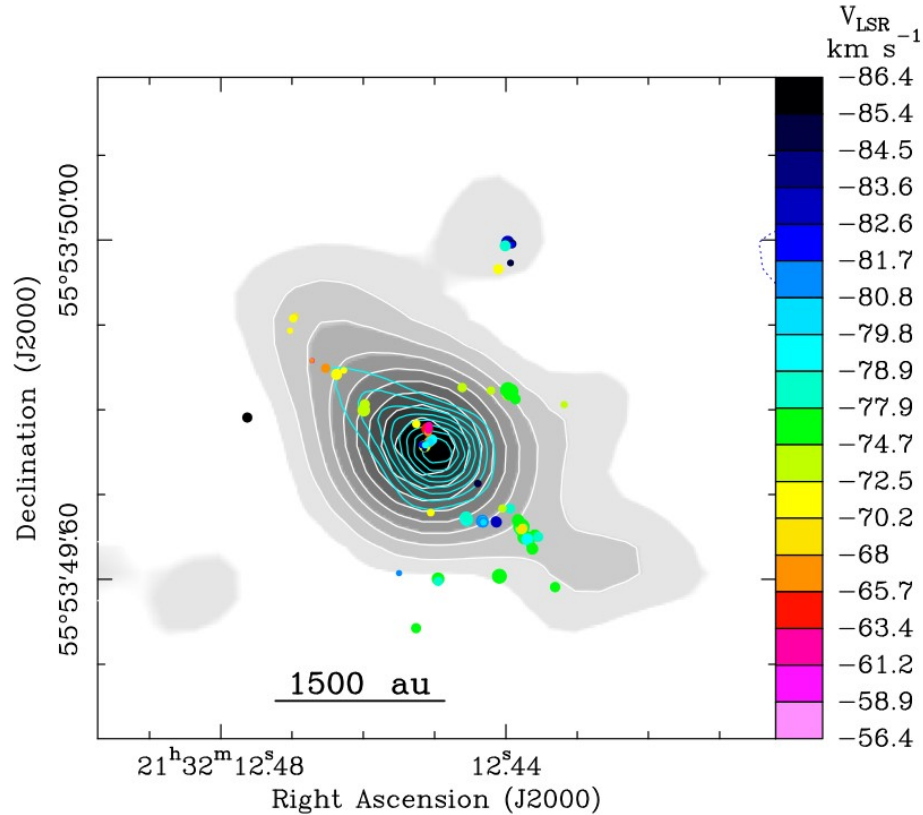
The ALMA observations of the high-mass star-forming region G10.34–0.14 reveal the existence of three massive hot cores.

The most massive of these cores, core S1, exhibits both high and low-velocity jet/outflow in the CO, SiO, and CH₃OH. It is associated with water and Class I methanol masers.

The core N shows a low-velocity CO outflow and is associated with an Extended Green Object, along with Class I and II methanol masers.

The characteristics of the outflows and masers in these two cores suggest they are in different stage of evolution and varying physical conditions.

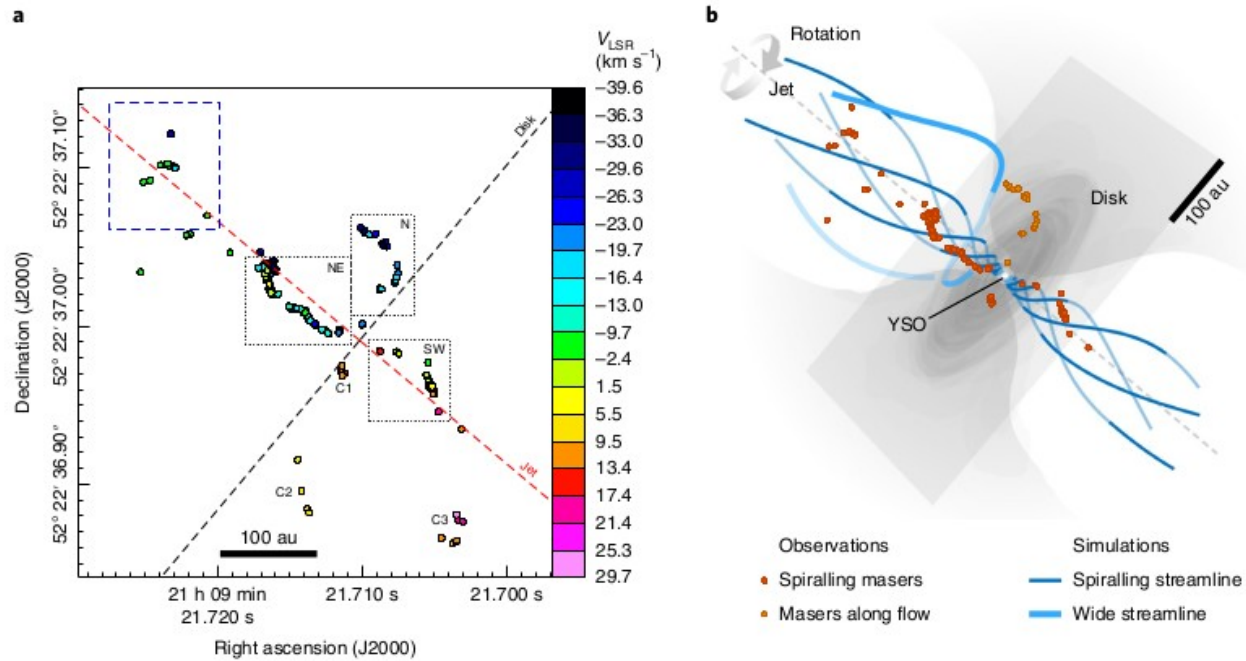
Series of works by Moscadelli, Sanna, Goddi:



Multifreq. and
multiepoch
observations.

Figure 1. Example of POETS observations for the target source G097.53+03.18. This map shows a typical combination of radio continuum emission, with grey shades and cyan contours for 12 and 22 GHz emission respectively, and 22.2 GHz water maser cloudlets, marked with colored dots according to the line-of-sight velocity scale to the right. Adapted from [Moscadelli et al. \(2016\)](#)

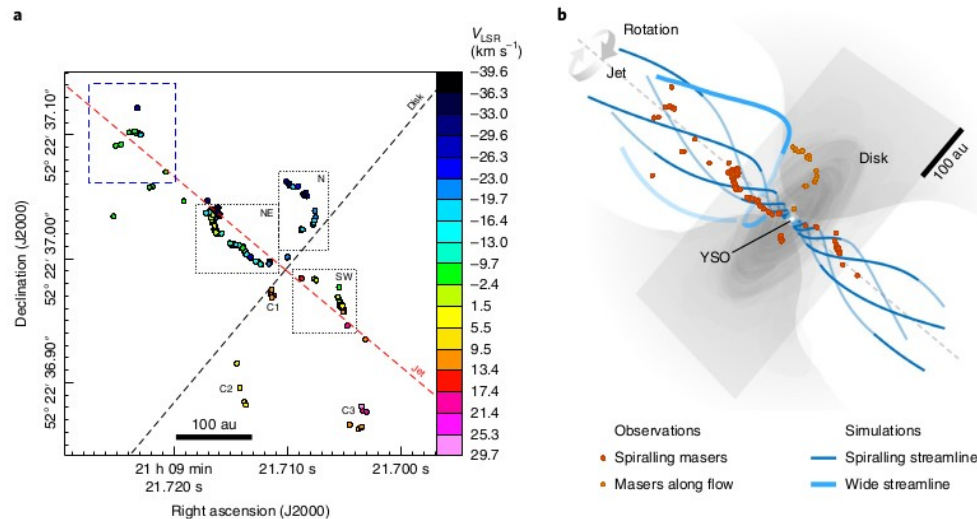
The magnetohydrodynamic disc wind in IRAS 1078+5211 – multi-epoch water maser (global) observations (Moscadelli et al. 2022)



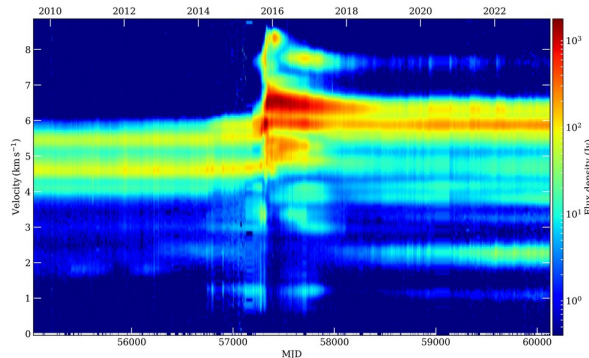
„Here we present a direct view of the velocity field of a disk wind around a forming massive star. Achieving a very high spatial resolution of about 0.05 au, our water maser observations trace the velocities of individual streamlines emerging from the disk orbiting the forming star.

We find that, at low elevation above the disk midplane, the flow co-rotates with its launch point in the disk, in agreement with magneto-centrifugal acceleration.

Beyond the co-rotation point, the flow rises spiralling around the disk rotation axis along a helical magnetic field.”

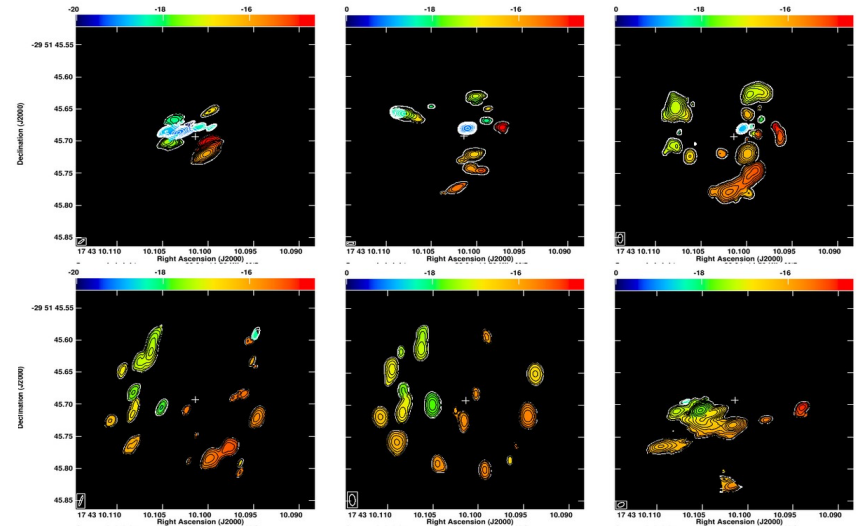
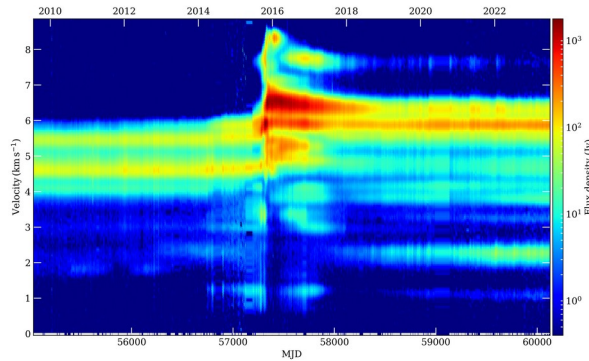


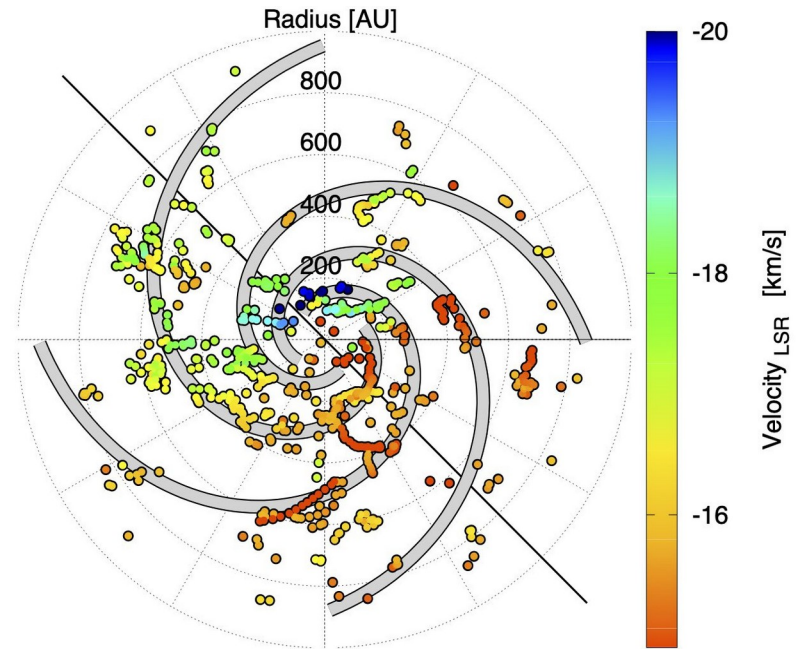
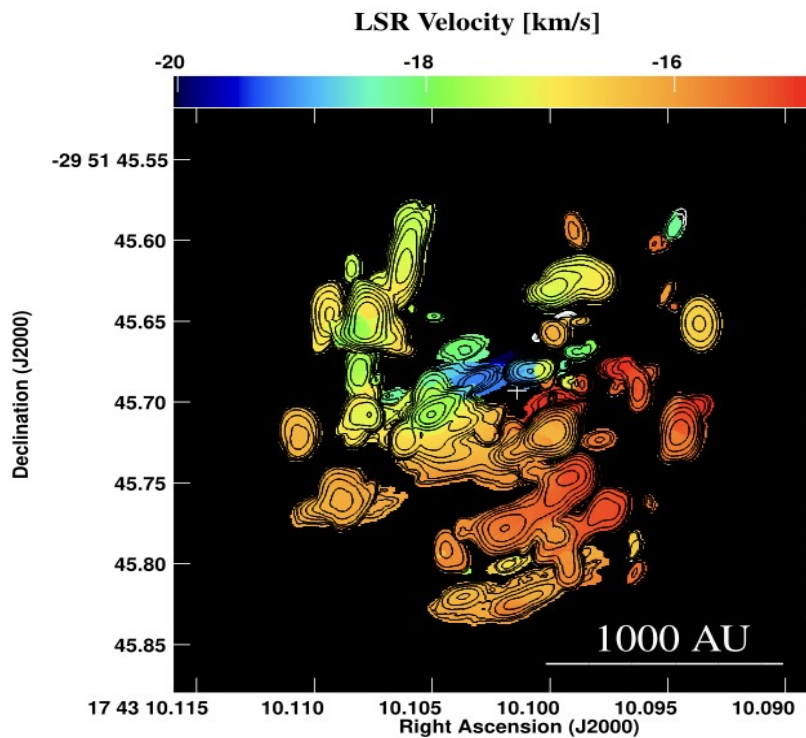
Episodic accretions (Meyer et al. 2017, 2020, 2021) confirmed!
All bursts of HMYSOs were preceded by 6.7 GHz methanol maser flares easily detected by single-dishes.



“A Keplerian disk with a four-arm spiral birthing an episodically accreting high-mass protostar” Ross et al. (2023, Nature Astronomy).

Episodic accretions confirmed!
All bursts of HMYSOs were preceded by 6.7 GHz methanol maser flares easily detected by single-dishes.

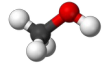




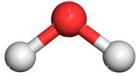
G358-MM1 has four spiral arms which wrap beautifully around the protostar. The spiral arms help to feed disk material down to the center of the system where it can reach the protostar and feed it.

Gray 2012: Maser emission is related to

- **Star formation**



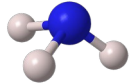
methanol (CH_3OH) – class I, II



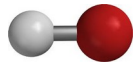
water (H_2O)



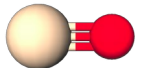
formaldehyde (H_2CO)



ammonia (NH_3)



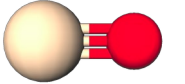
hydroxyl (OH)



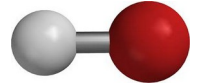
silicon monoxide (SiO)

- **Evolved stars (AGB, RSG)**

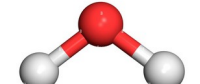
silicon monoxide (SiO)



hydroxyl (OH)

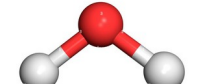


water (H_2O)

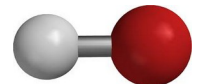


- **Planetary nebulae and pPN**

water (H_2O)



hydroxyl (OH)



Evolved stars: Water fountains

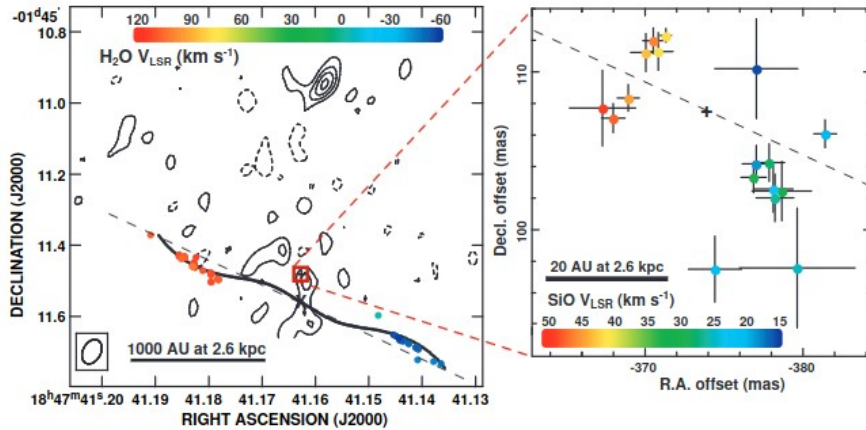
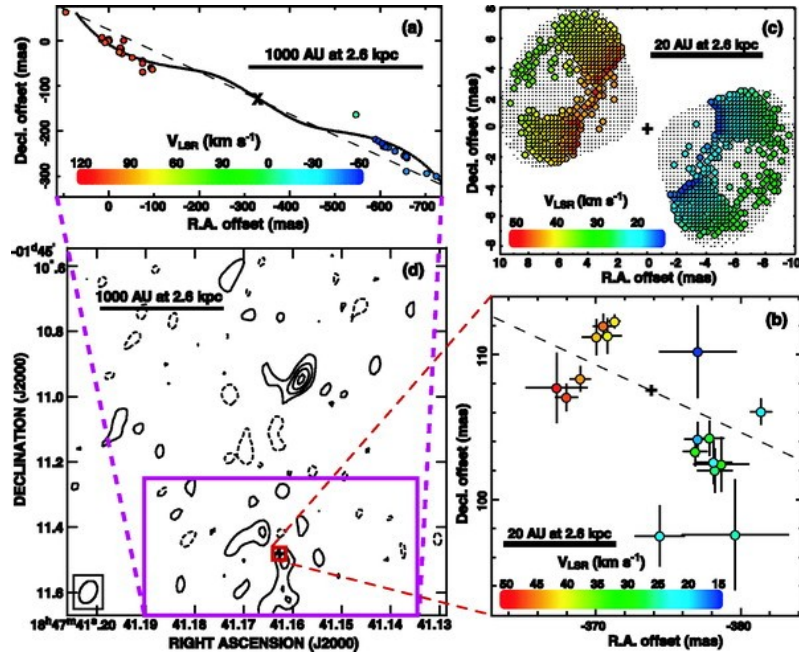


Figure 1. H₂O, SiO ($v=1, J=1-0$) maser emission, and 7 mm continuum emission in W43A. Different colors denote maser features' line-of-sight velocities, according to the color scale. *Left* Spatio-kinematics of the H₂O maser features observed on 2002 April 3. A dotted line shows a pattern of a precessing jet appearing in the year 2002.3, which is modeled by [Imai et al. 2002](#). A symbol "X" indicates the dynamical center of the modeled jet. A thin dashed line indicates the axis direction of the H₂O maser jet. *Right* Spatio-kinematics of the SiO maser features. Horizontal and vertical bars of individual maser features indicate uncertainties of feature positions in R.A. and decl. directions, respectively. A plus symbol indicates a roughly-estimated location of the dynamical center of the biconically-expanding flow found in the SiO maser kinematics. Roughly a flux density of a spot is inversely proportional to an error bar of the spot.

- Water fountain (WF) objects are generally **defined as evolved stars with low to intermediate initial mass accompanied by high-velocity molecular jets detectable in the 22.235 GHz H₂O maser line.**
- They are the key objects of understanding the morphological transitions of circumstellar envelopes during the post asymptotic giant branch phase. Masers are useful tools to trace the kinematic environments of the circumstellar envelopes.

Imai et al. 2007

Evolved stars: Water fountains

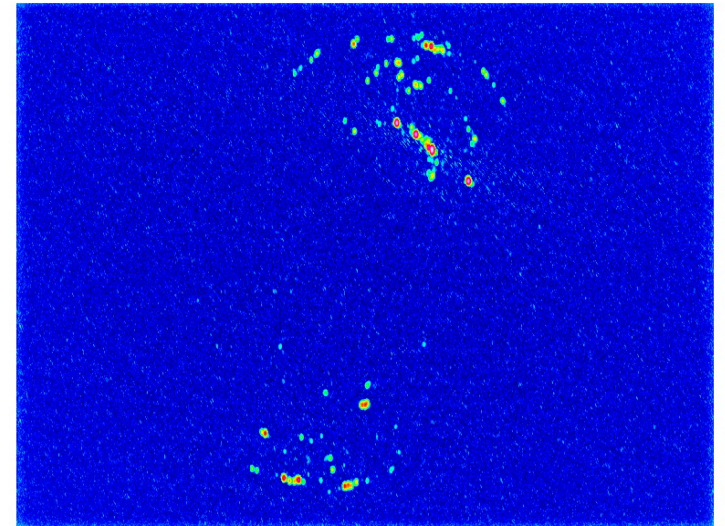
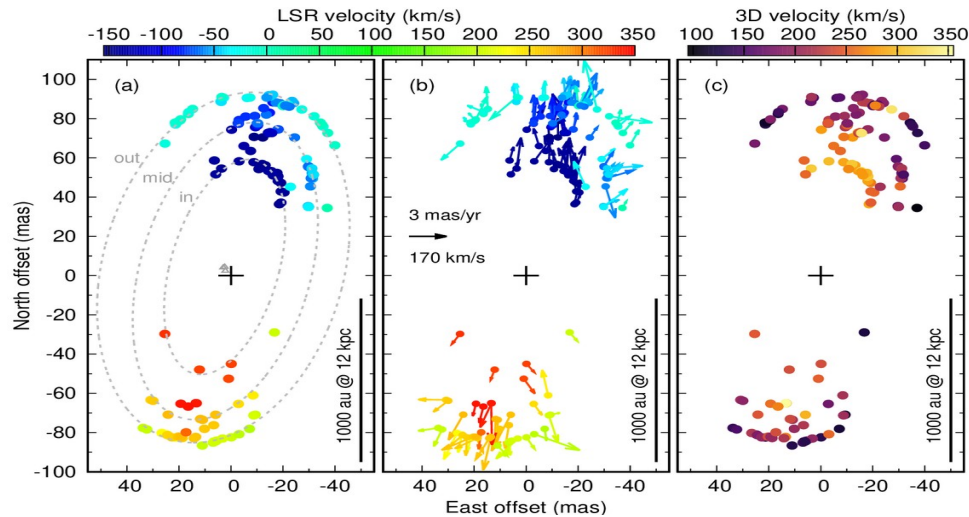


- The H₂O maser emission traces significantly faster motions than the typical expansion velocities of circumstellar envelopes (CSEs) during the AGB phase (10–30 km/s).
- The short dynamical ages of the maser jets (5–100 yr) may indicate that WFs represent one of the first manifestations of collimated mass-loss in evolved stars.
- Water Fountains, located between the AGB and PN phases of stellar evolution, may provide significant clues on the shaping process of PNe.

Imai et al. 2005: A Biconically Expanding Flow in W43A Traced by **SiO Maser Emission**.

Tracing outflows in AGB stars

Orosz et al. (2018): 22 GHz water fountain at **post-AGB star** IRAS 18113-2503 with spectacular bipolar bow shocks in its high-speed collimated jet-driven outflow. **The jets are formed in very short-lived, episodic outbursts, which may indicate episodic accretion in an underlying binary system.** VLBA observations.



Ouyang et al. 2024 - **Excited-state OH** Masers in the Water Fountain Source IRAS 18460-0151

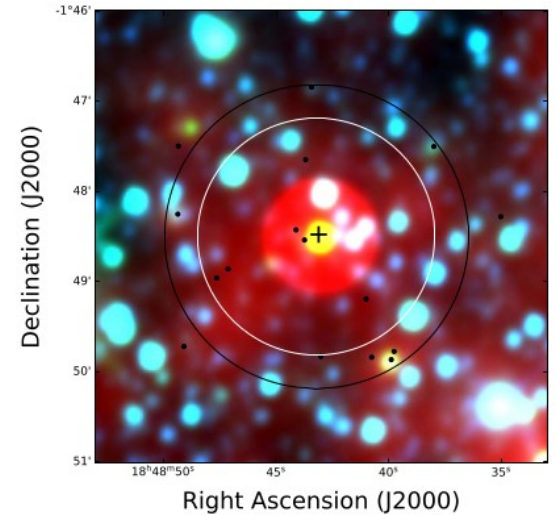
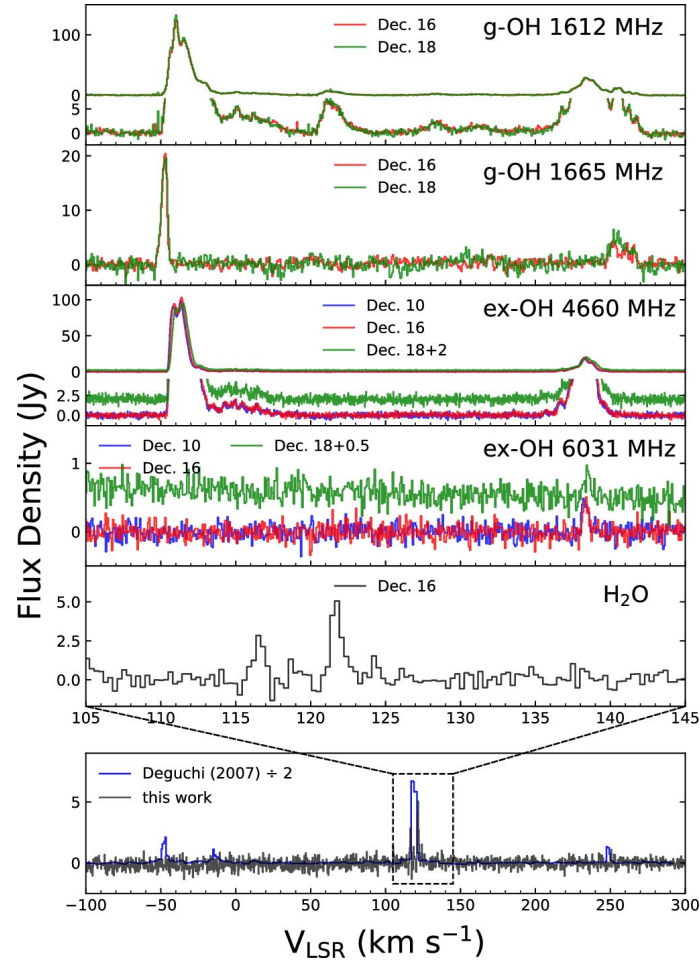
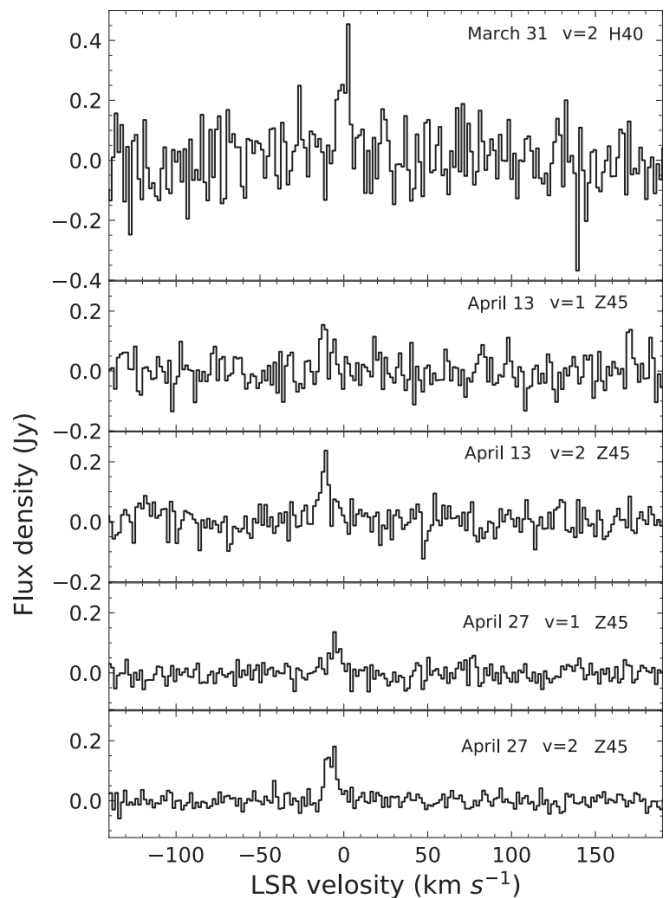


Figure 2. The WISE image of I18460. The 3.4, 4.6, and 22 μm bands are shown in blue, green, and red, respectively. The white and black circles indicate the beam sizes of TMRT at 6.0 and 4.7 GHz, respectively, and the cross marks the position of the beam center. The dots denote the surrounding young stellar objects.

Kei Amada et al. 2024 – Discovery of SiO masers in the Water Fountain source IRAS 16552–3050



- We report new detections of SiO $v = 1$ and $v = 2$ $J = 1 \rightarrow 0$ masers in WF IRAS 16552-3050, which was observed with the Nobeyama 45 m telescope from March 2021 to April 2023. The 2nd case of WF with SiO masers!
- The line-of-sight velocity of the SiO masers are blue-shifted by $\sim 25 \text{ km s}^{-1}$ from the systemic velocity. This velocity offset imply that the SiO masers are associated with nozzle structure formed by a jet penetrating the circumstellar envelope, and that new gas blobs of the jet erupted recently. Thus, **the SiO masers imply this star to be in a new evolutionary stage.**

Uscanga et al. 2024: Evolution of the outflow traced by water masers in the evolved star IRAS 18043–2116

„We estimate that the spatial separation of the two main clusters of H₂O masers has doubled (45 mas vs 88 mas) in a period of about 12.5 yr. Interestingly, the new highest velocity components possibly located at the outer outflow lobes are farther away from the center, indicating **a rapid growth of the outflow triggered by an increase in the maximum outflow velocity.**”

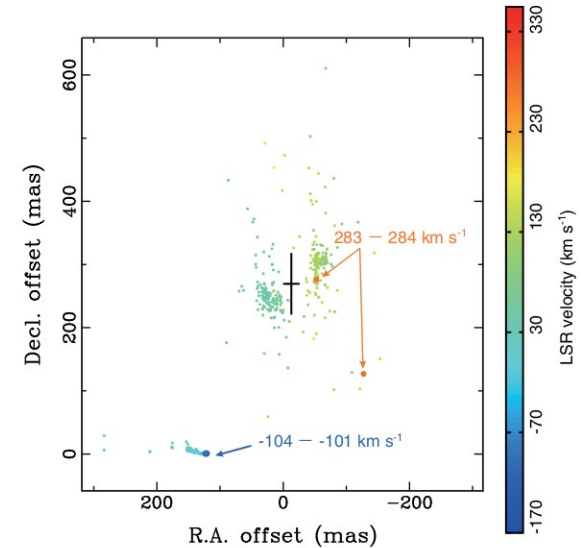
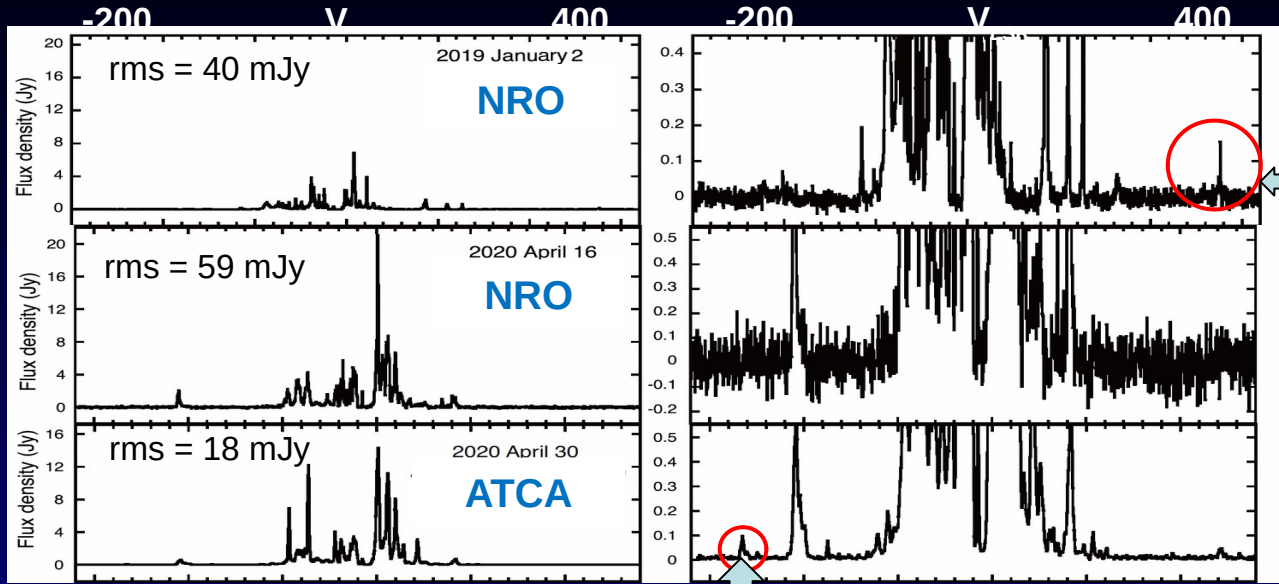


Figure 2. Map of H₂O masers in I18043 taken with ATCA on 2021 March 30. The maser distribution has a larger positional uncertainty in declination offset (up to 200 mas). The new blue-shifted components ($V_{\text{LSR}} \sim -102 \text{ km s}^{-1}$) and the red-shifted components ($V_{\text{LSR}} \sim 284 \text{ km s}^{-1}$) are highlighted in bigger filled circles. The position and the size of a black cross indicate the position and statistical error (3σ) of the continuum source. The synthesized beam is $1.42 \text{ arcsec} \times 0.41 \text{ arcsec}$ at a position angle of -1.27° (Uscanga *et al.* 2023).

New highest velocity components of the H₂O masers in the WF IRAS 18043-2116



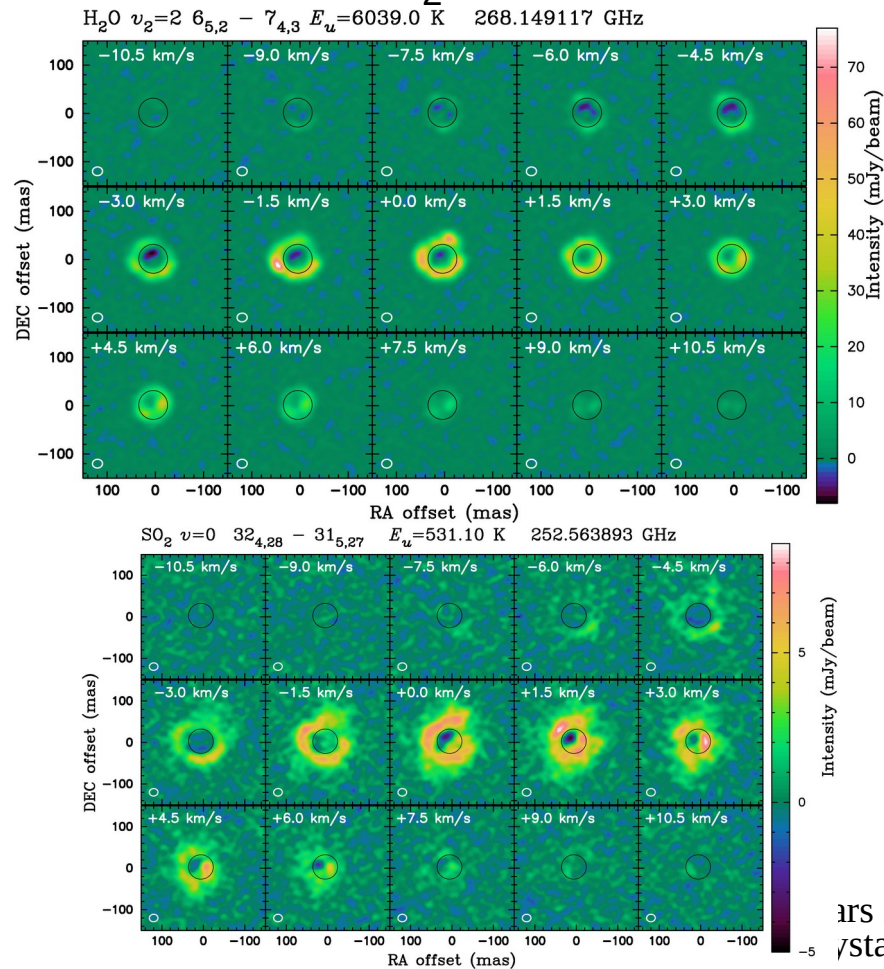
376 km/s

Largest velocity spread km/s

Uscanga+ 2023

165 km/s

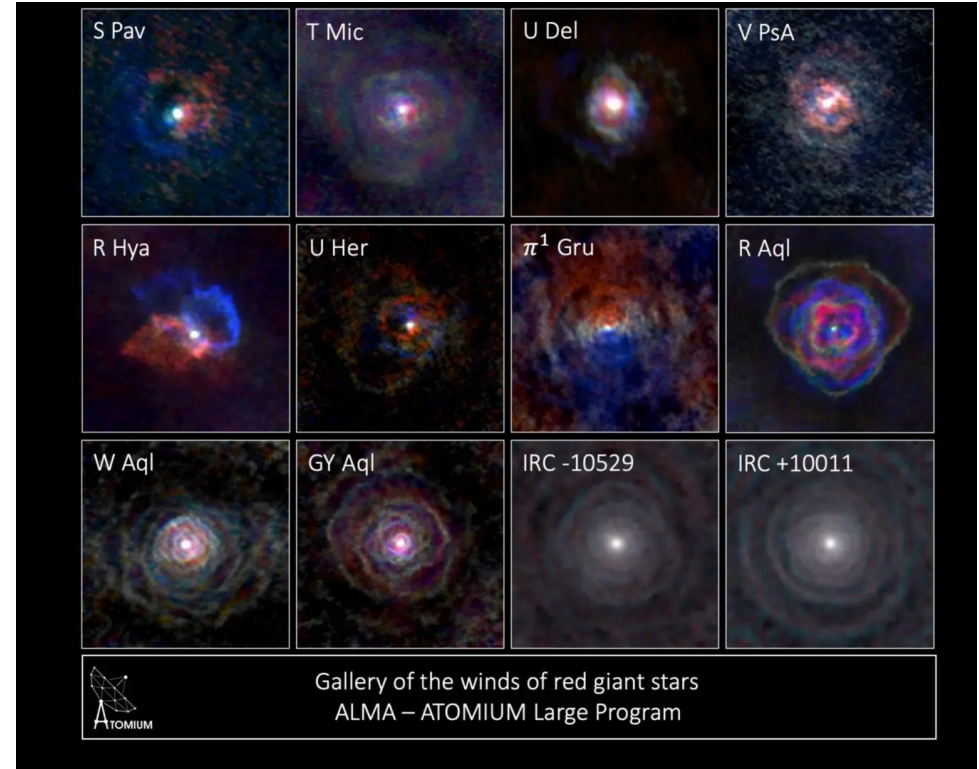
Ohnaka et al. 2024 - High resolution ALMA imaging of H₂O, SiO, and SO₂ masers in the atmosphere of the AGB star W Hya



- To shed light on the long-standing problem of mass loss from AGB stars, it is indispensable **to probe the region within a few R^* , where dust forms and the wind accelerates**. We focus on the well-studied oxygen-rich AGB star W Hya.
- 20-milliarcsecond resolution ALMA imaging of the well-studied AGB star W Hya in multiple molecular lines at 250–269 GHz, including masers from SiO, H₂O, and (SO₂?).
- The maser emission is confined within a radius of ~ 50 mas ($= 2.4 R^*$). It may trace pockets of dense, cool regions in the inner wind of oxygen-rich stars, where dust formation can take place.

ATOMIUM – talk by Carl Gottlieb

- The ATOMIUM project aims to learn more about the physics and chemistry of old stars. *„Cool aging stars are considered boring, old and simple, but we now prove that they are not: they tell the story of what comes after.”*



ATOMIUM

- First detection of a new companion and its effect on the inner wind - the SiO masers appearing to trace a flow towards the companion in AGB star π^1 Gruis ($1.1 M_{\text{Sun}}$).

(Homan et al. 2020)

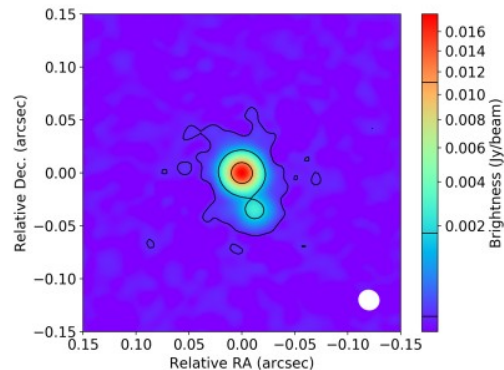


Fig. 1. Continuum emission of the π^1 Gru system, as observed by the extended 12 m configuration, at 211–275 GHz. Contours are drawn at 3, 120, and 768 times the continuum rms noise value (1.5×10^{-5} Jy beam $^{-1}$). The ALMA beam size is shown in the bottom right corner. The continuum shows a second peak to the south-west of the central emission.

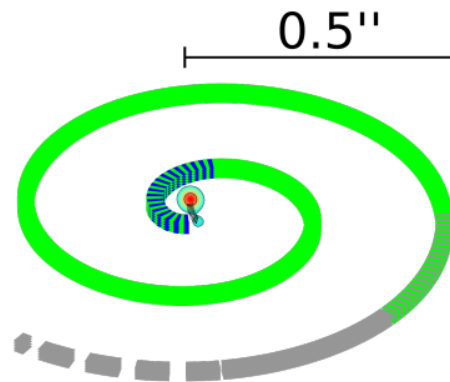
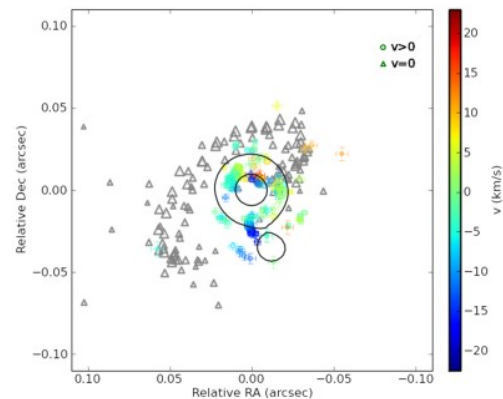
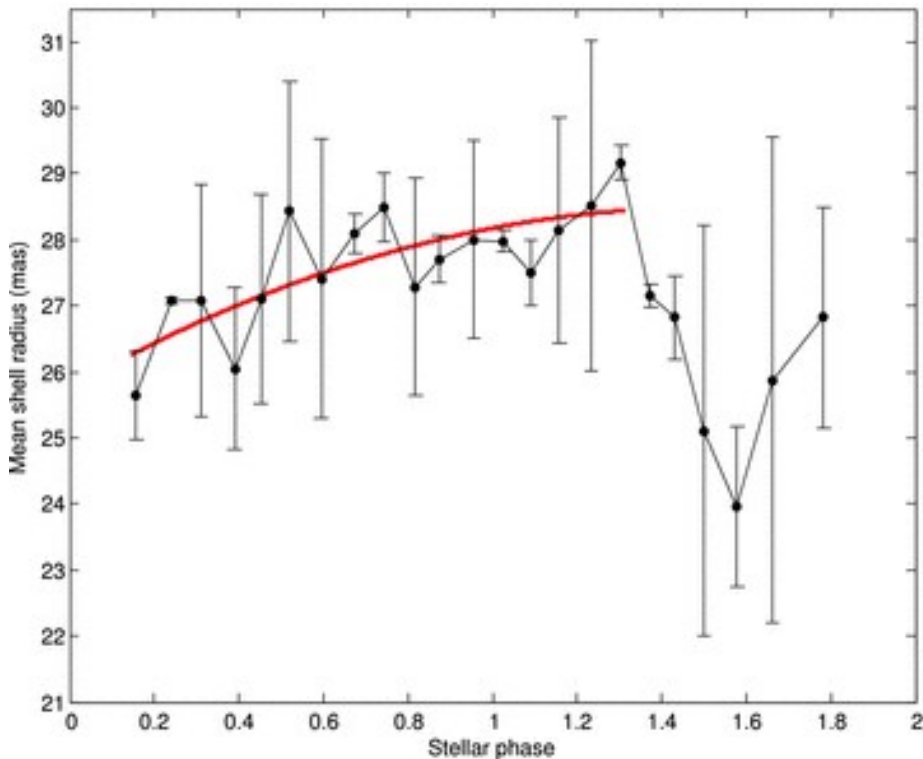
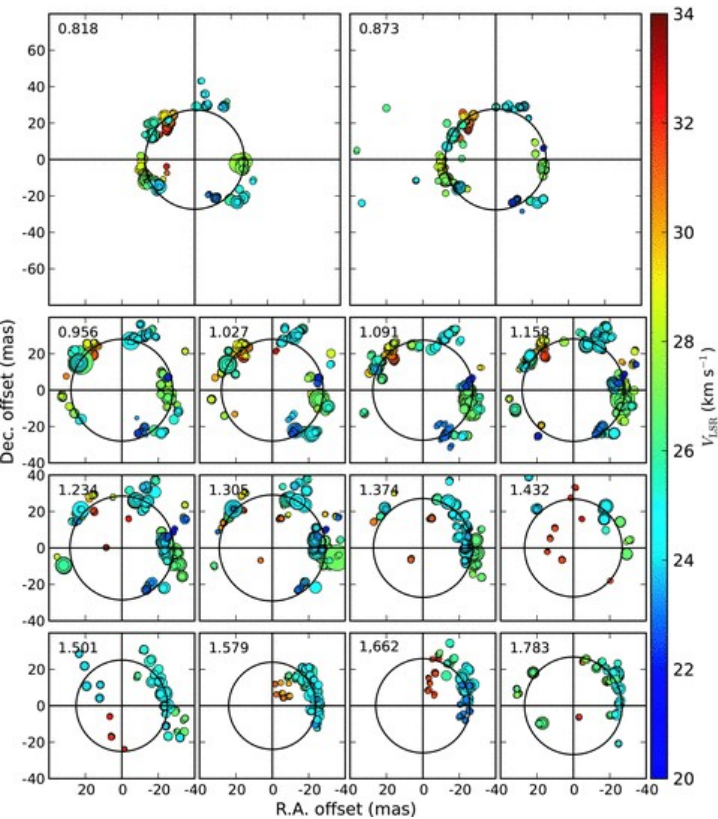


Fig. 13. Schematic diagram of the inner wind of π^1 Gru. In the center is a cut-out of the $120\sigma_{\text{rms}}$ contour of the ALMA continuum, from which the inclined spiral is launched. The colours of the spiral represent the different diagnostics used: blue is the SiO, green is the HCN, grey is the CO emission, and black is the stream of accelerating gas probed by the maser emission. The dashes parts represent regions of overlap.



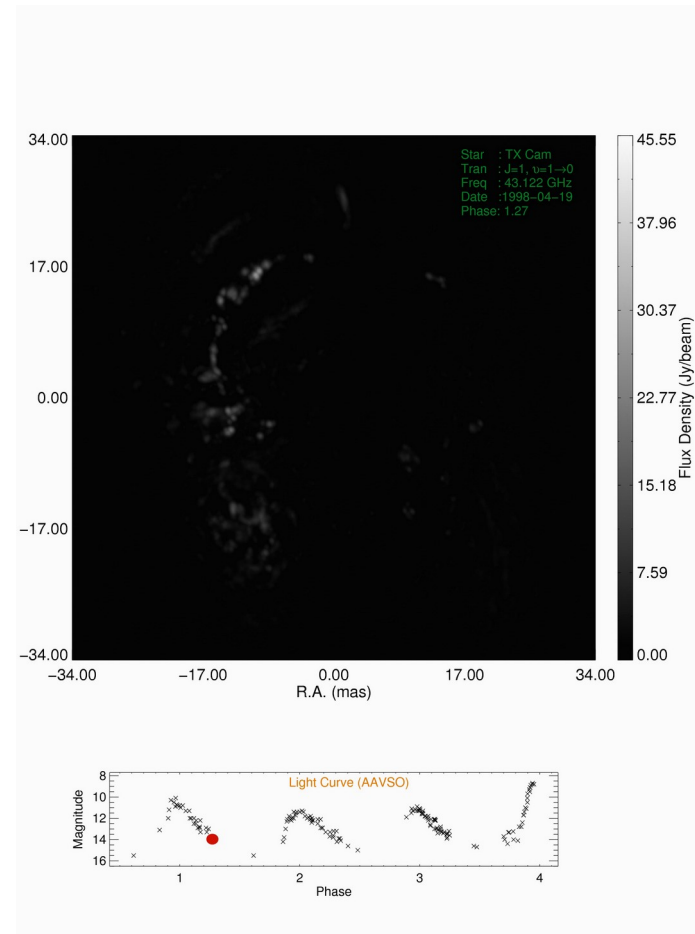
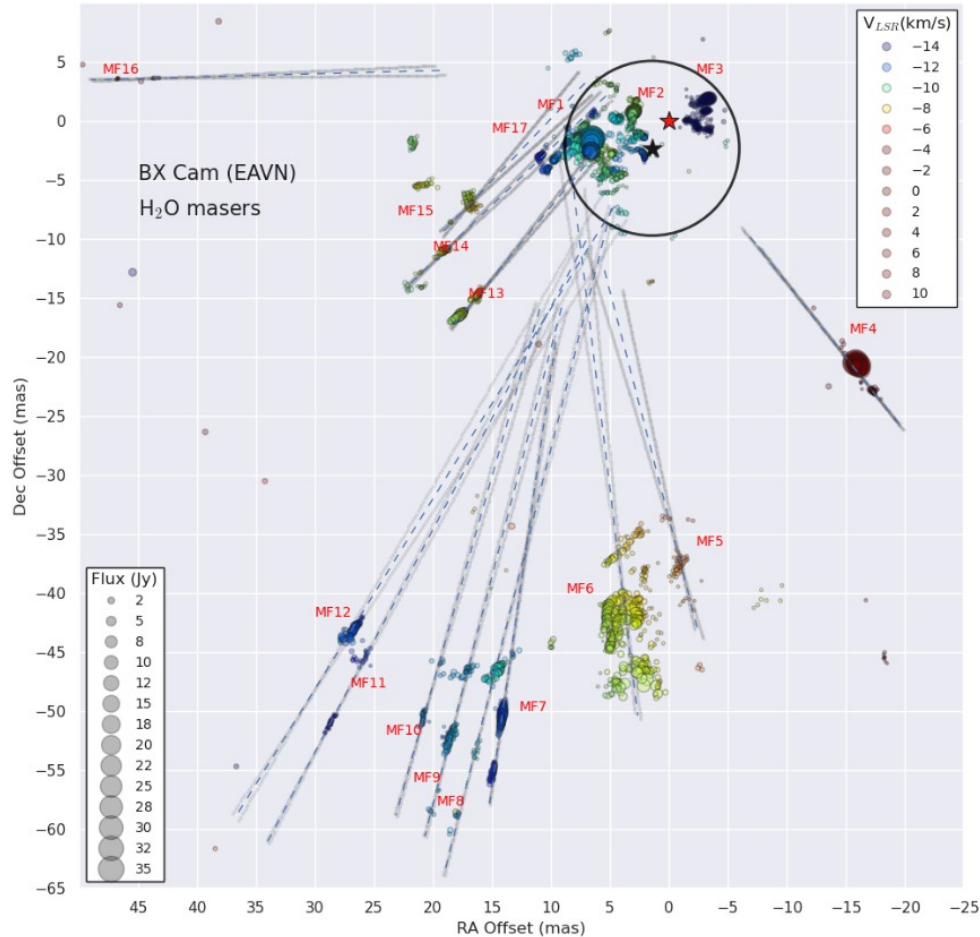
Assaf et al. 2011: The 43-GHz SiO maser in the circumstellar envelope of the asymptotic giant branch star R Cassiopeiae

Total intensity images of the SiO maser emission towards R Cas centred on the star at a radius of $1.6\text{--}2.3R^*$.



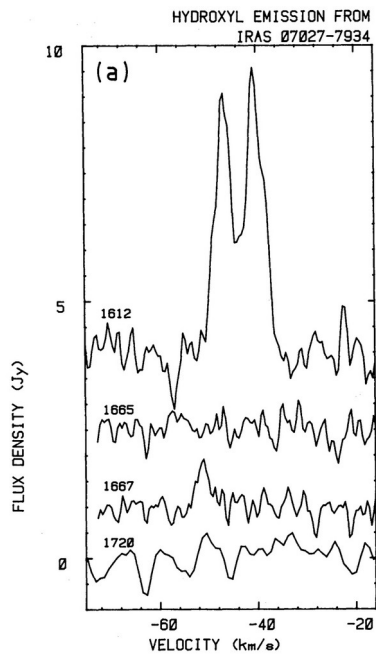
- The variation of the SiO maser ring radius with the stellar phase.
- The infall time towards the star is greater than the pulsation period with a factor of ~ 1.2 .

The Astrometric Animation of Water Masers towards the Mira Variable BX Cam – Xu et al. 2022, 2024

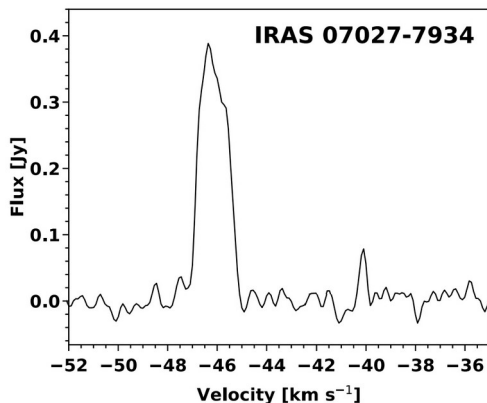


Gonidakis, Diamond & Kemball (2013): 112 frame movie, showing the evolution and global kinematics of the SiO masers towards TX Cam.

Cala et al. 2024 – Nascent planetary nebulae: new identifications and extraordinary evolution



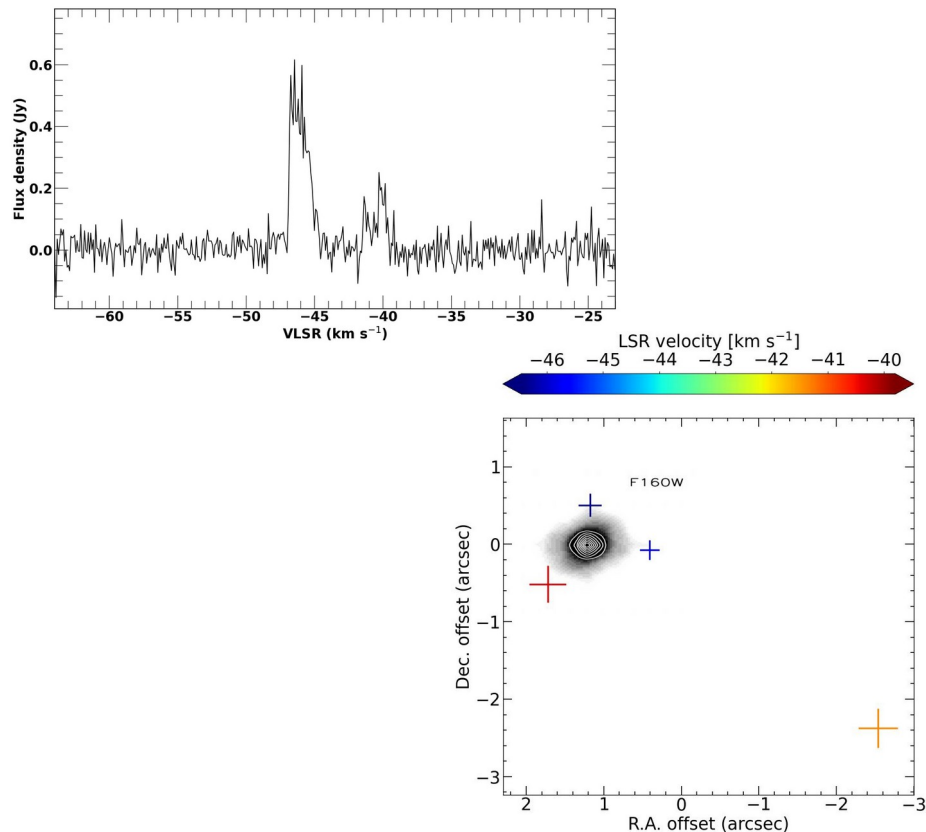
Zijlstra et al. 1991



A single 1612 MHz OH blueshifted maser component is common among maser-emitting planetary nebulae, and has been interpreted as the far side receding redshifted maser component being absorbed by an optically thick photoionized nebula. Hence, in IRAS 07027-7934, the fading of the redshifted maser emission is consistent with the nascent and early expansion of the photoionized nebula, since, the onset of the photoionization marks the end of the post-AGB, and the beginning of the planetary nebula phase.

- Planetary nebulae (PNe) harbouring masers of H₂O (H₂OPNe) and/or OH (OHPNe) are thought to be nascent PNe.
- **We found variability in the 1612 MHz OH spectra of IRAS 07027-7934, which could be related to the expansion of a nascent photoionized region consistent with the onset of the PN phase.**

Cala et al. 2024 – Nascent planetary nebulae: new identifications and extraordinary evolution



The spatial distribution of the two brightest blueshifted maser components, and the redshifted components at -41.4 and -40.3 km/s. In addition, it has overlaid a broadband (F160W) HST image centered at 1.6 μ m, which traces photoionized gas, and a contour map of the carbon-rich dust emission from ionized PAHs (García-Hernández et al. 2006), where we have assumed that the position of the central star of IRAS 07027-7934, which has been spectroscopically classified as carbon-rich (Menzies & Wolstencroft 1990) and lies at the same position of the peak emission of the contour map, also lies between the brightest maser components. Anyways, given that the entire size of the circumstellar nebula seen by means of scattered H α light is \sim 15 arcsec (Zijlstra et al. 1991), thus the spatial distribution of the OH masers confirms that these masers are located farther away from the central star than the PAHs, as well as that IRAS 07027-7934 was an oxygen-rich AGB that evolved into a carbon-rich central star.

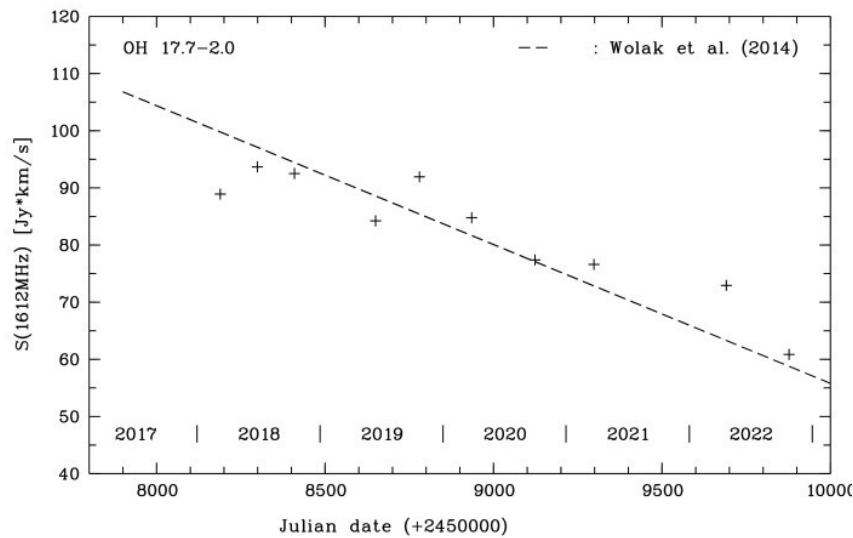
Etoka et al. 2024: The loss of OH maser emission in the early stage of Post-AGB evolution

Based on the results of an on-going monitoring program of 1612 MHz OH masers in OH/IR stars, we determined a lifetime encompassing late AGB and early post-AGB evolution of at least 4500 years. Fading of the OH masers observed with the Nançay Radio Telescope is detected in several post-AGB OH/IR stars on timescales of decades, while AllWISE/NEOWISE light curves taken almost in parallel show diverse behaviours.

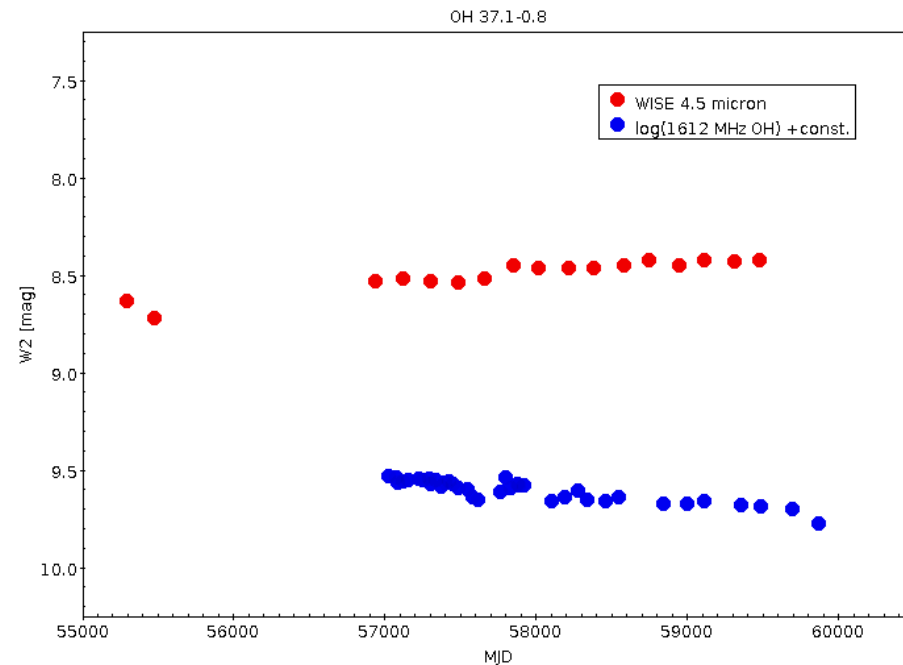
Our results do not show a clear correlation between the fading OH and long-term infrared brightness variations. However, the long-term variations show that stellar evolution in the AGB to post-AGB transition phase can be observed in real time.



Etoka et al. 2024: The loss of OH maser emission in the early stage of Post-AGB evolution



The maser disappearance in OH 17.7-2.0.



The correlation between the OH & IR for the "well-behaved" OH 37.1-0.8.

Envelopes



- Engels et al. 2024: Compilation of galactic stellar sources observed for OH maser emission in the transition at 1612, 1665, and 1667 MHz. Extension to H₂O and SiO maser emission is in progress. **The database contains 16879 OH maser observations at frequencies 1612, 1665, and 1667 MHz selected from the literature.**
- <https://hsweb.hs.uni-hamburg.de/projects/maserdb/>

MaserDB

<https://maserdb.net/>

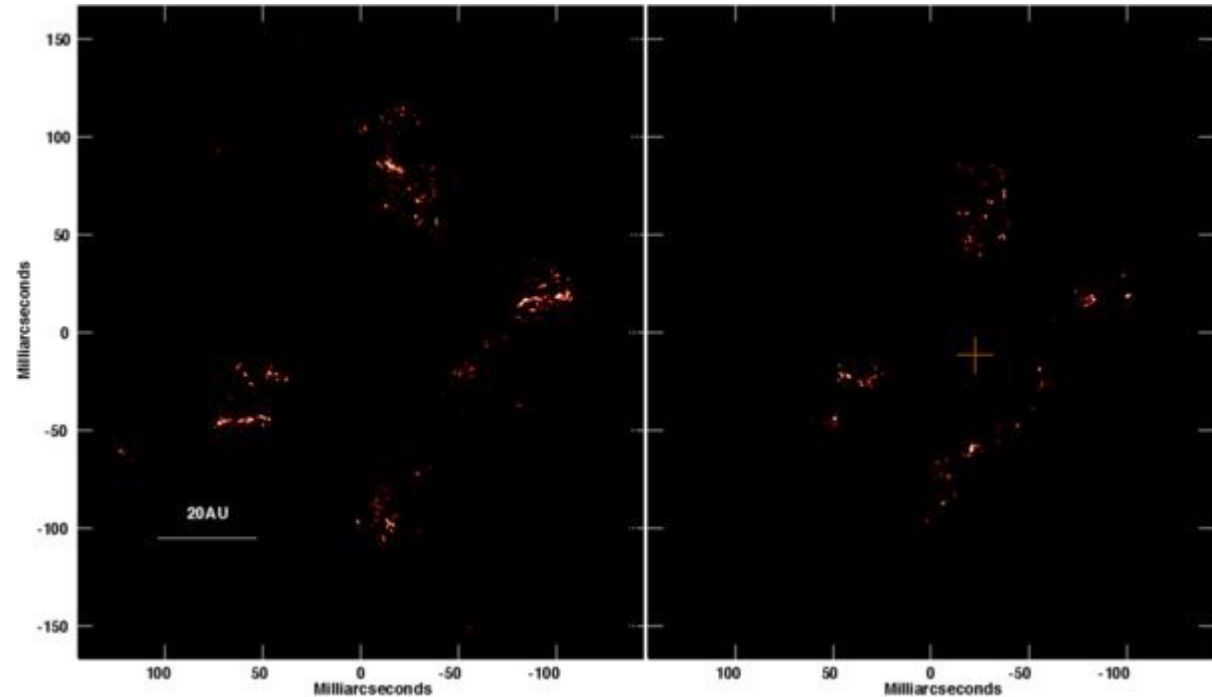


- The importance of long term monitoring.
- Multifrequency and multiepoch observations are needed.
- An example:

- The importance of long term monitoring.
- Multifrequency and multiepoch observations are needed.
- An example:

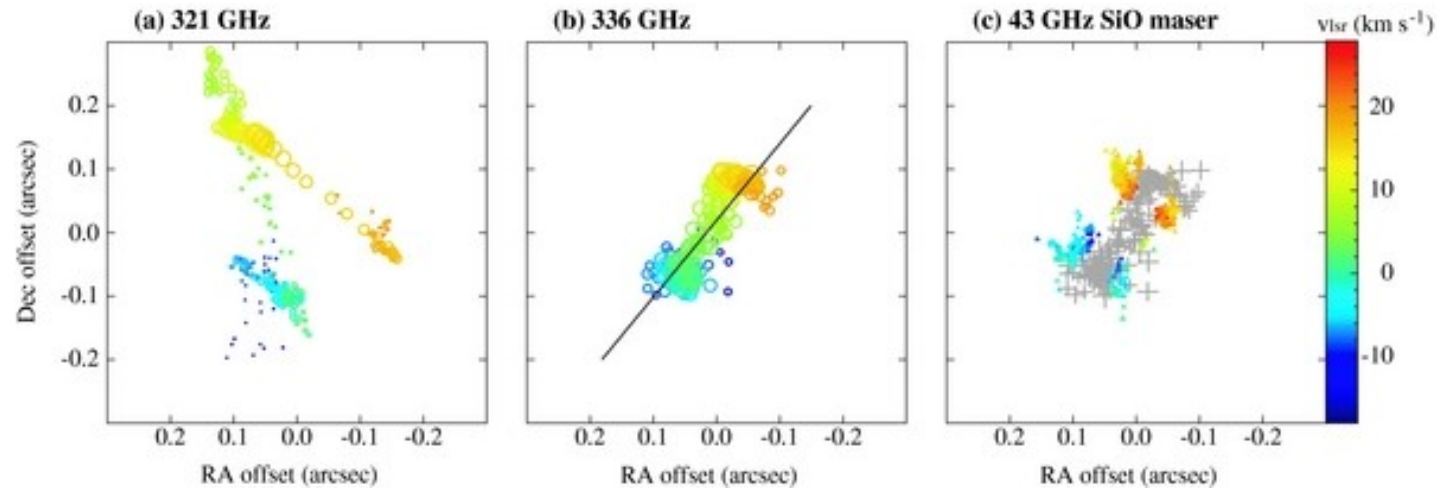
Orion Source I

(Matthews et al. 2010)

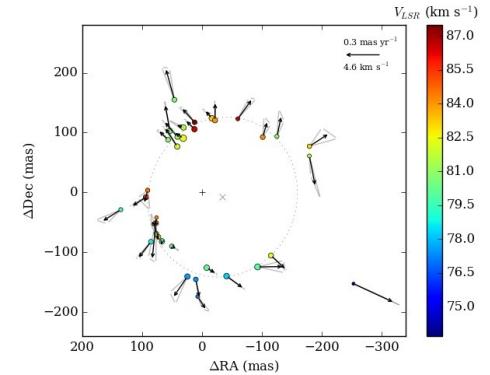
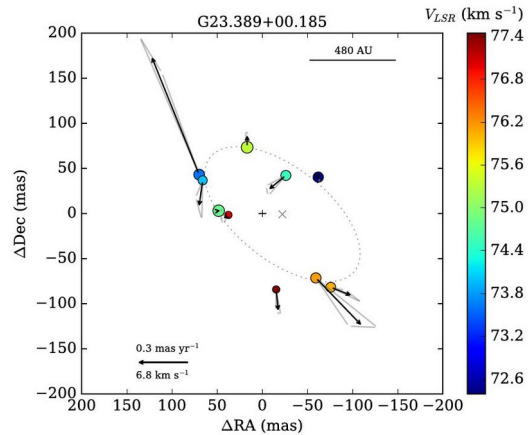
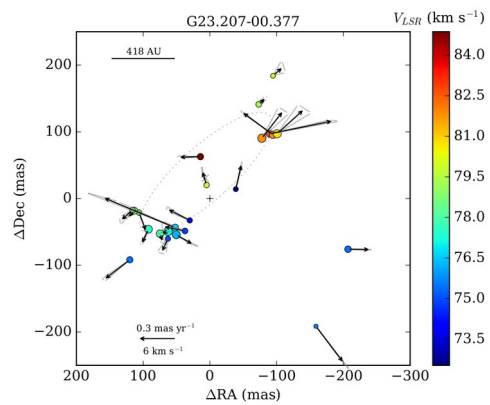


- The importance of long term monitoring.
- Multifrequency and multiepoch observations are needed.
- An example:

Orion Source I
(Hirota et al. 2014)



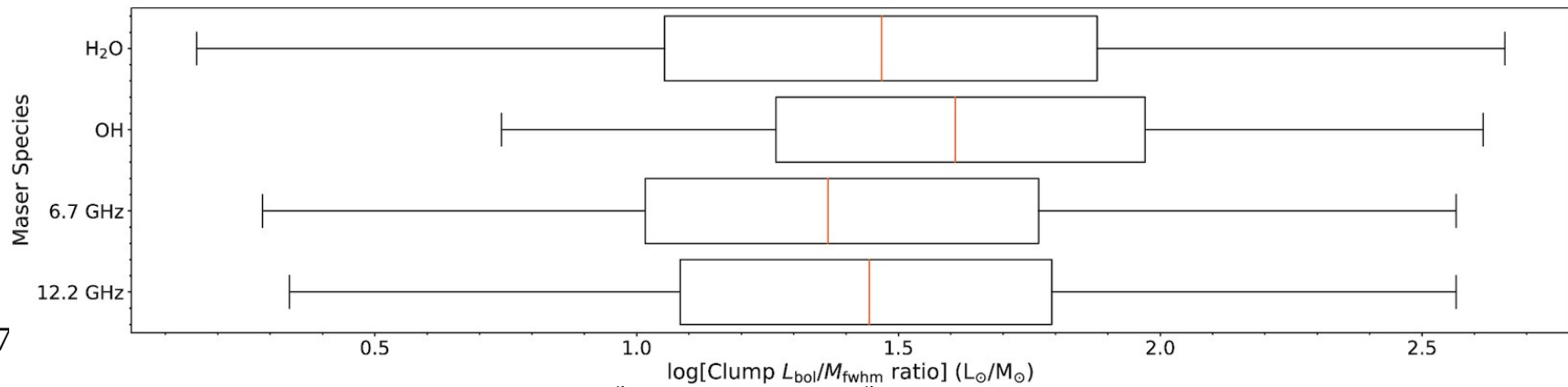
- The importance of long term monitoring.
- Multifrequency and multiepoch observations are needed.
- An example: methanol maser rings in HMSFRs (Bartkiewicz et al. 2020, 2024)



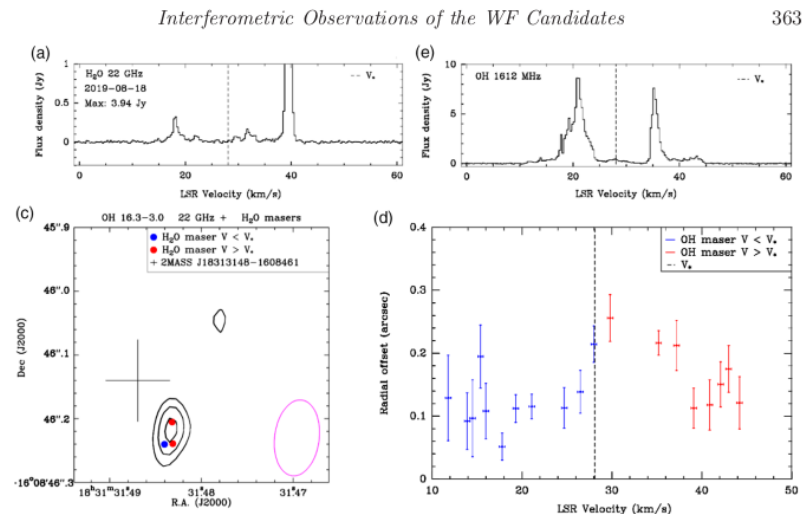
- Billington et al. 2020: „We have used catalogues from several Galactic plane surveys and dedicated observations to investigate the relationship between various maser species and Galactic star-forming clumps, as identified by the ATLASGAL survey. The maser transitions of interest are the 6.7 and 12.2-GHz methanol masers, 22.2-GHz water masers, and the masers emitting in the four ground-state hyperfine structure transitions of hydroxyl.”

„**The conditions required for the production of maser emission only occur during a relatively narrow period during a star’s evolution.**”

- Statistical lifetimes are calculated for the water, hydroxyl and 12.2-GHz methanol masers, and these lifetimes are found to be $\sim 1.6, 0.4,$ and 2.0×10^4 yr, respectively. We find that the lifetimes for the 6.7-GHz (as found in Billington et al. 2019) and 12.2-GHz methanol masers **are in good agreement with the values predicted by Breen et al. (2010), whereas the statistical lifetimes determined for the water and hydroxyl masers are considerably shorter than those predicted, by one quarter and one half, respectively.** The lifetimes calculated for all masers are a lower limit on the true lifetimes, and so, our results support the ‘straw man’ model (Ellingsen et al. 2007).



Chacón et al. 2024: Interferometric Observations of the Water Fountain Candidates OH 16.3–3.0



- The spatial distribution of the H₂O maser components (Fig. 1c) does not show conclusive evidence for a collimated jet. It is still possible that the source is a WF, but with the outflow lying close to the plane of the sky, or a different kind of WF, e.g., with a less massive progenitor or with a relatively younger age

Figure 1. VLA observations toward the WF candidate OH16.3. (a) H₂O maser spectrum, zoomed in to better show the faint emission components. (b) OH maser spectrum. It shows a double-peaked profile with prominent wings. (c) Contour map of the radio continuum emission at 22 GHz. The contours are 3,4,5 times 1.3×10^{-5} Jy beam⁻¹. The positions of the H₂O maser components are indicated by blue and red dots according to their velocities. The relative positional uncertainty between the H₂O masers is < 3.5 mas. The size of the cross of the 2MASS position indicates its 1σ position error. The magenta ellipse shows the synthesized beam. (d) V - R diagram of OH16.3. Since the stellar position does not coincide with the center of the spatial distribution of the OH masers, we considered the intensity-weighted emission centroid of the OH maser positions as the zero radial offset. The dashed lines indicate the assumed stellar velocity (V_*).

Baudry et al. 2024 – ALMA Large Program called ATOMIUM: ALMA tracing the origins of molecules in dust-forming O-rich M-type stars

- 14 Asymptotic Giant Branch (AGB) stars and three Red Supergiants (RSGs) aiming at understanding the chemistry of the dust precursors as well as the links between chemistry and the wind dynamics of these stars; see first results in e.g., Decin et al. (2020), Gottlieb et al. (2022), Baudry et al. (2023).

Baudry et al. 2023 – ATOMIUM: Probing the inner wind of evolved O-rich stars with new, highly excited H₂O and OH lines

- Water (H₂O) and the hydroxyl radical (OH) are major constituents of the envelope of O-rich late-type stars. Transitions
- involving energy levels that are rotationally or vibrationally highly excited (energies >4000 K) have been observed in both H₂O and
- OH.
- **Thermal and masing lines observations**

Pimpanuwat et al. 2024: Investigating the inner circumstellar envelopes of oxygen-rich evolved stars with ALMA observations of high-J SiO masers

- We highlight a few results from ALMA Band 6 observations of high-rotational transition number (J) SiO masers towards oxygen-rich AGB and red supergiant stars carried out as part of the ATOMIUM Large Programme in 2018–2020.
- A search for a relationship between mass-loss rates and flux-weighted mean angular distances of maser components was inconclusive, as linear regression models for the 28 SiO $v=1$ J=5–4 and J=6–5 transitions were inconsistent. Supplementary APEX observations towards the ATOMIUM AGB stars also suggest variability at different stellar pulsation phases.